UNITED STATES
NUCLEAR REGULATORY COMMISSION
Washington, D.C. 20555

April 1, 1986

## ERRATA SHEET

Report Number: NUREG/CR-4503
ANL-86-3

Report Title: Long-Term Embrittlement of Cast Duplex Stainless Steels in LWR Systems: Annual Report, October 1984-September 1985

Prepared by: Argonne National Laboratory

Date Published: January 1986

Instructions: Report was printed with an incomplete NUREG/CR identification number. Please correct your copy to read as follows:

NUREG/CR-4503, Vol. 1

Division of Technical Information
and
Document Control

8604180327 860131
PDR NUREG
CR-4503 R PDR

Materials Science and Technology Division

NUREG/CR-4503
ANL-86-3

# Long-term Embrittlement of Cast Duplex Stainless Steels in LWR Systems:

## Annual Report October 1984–September 1985

by O. K. Chopra and H. M. Chung

Argonne National Laboratory, Argonne, Illinois 60439
operated by The University of Chicago
Prepared for the Office of Nuclear Regulatory Research
U. S. Nuclear Regulatory Commission under Interagency Agreement DOE 40-550-75

Argonne National Laboratory, with facilities in the states of Illinois and Idaho, is owned by the United States government, and operated by The University of Chicago under the provisions of a contract with the Department of Energy.

**NOTICE**

This report was prepared as an account of work sponsored by an agency of the United States Government. Neither the United States Government nor any agency thereof, or any of their employees, makes any warranty, express or implied, or assumes any legal liability or responsibility for any third party's use, or the results of such use, of any information, apparatus, product or process disclosed in this report, or represents that its use by such third party would not infringe privately owned rights.

Available from

Superintendent of Documents
U. S. Government Printing Office
Post Office Box 37082
Washington, D.C. 20013-7982

and

National Technical Information Service
Springfield, VA 22161

NUREG/CR-4503
ANL-86-3
(Distribution
Code: R5)

ARGONNE NATIONAL LABORATORY
9700 South Cass Avenue
Argonne, Illinois 60439

# LONG-TERM EMBRITTLEMENT OF CAST DUPLEX STAINLESS STEELS IN LWR SYSTEMS:

## ANNUAL REPORT
October 1984—September 1985

by

O. K. Chopra and H. M. Chung

Materials Science and Technology Division

Report Completed
January 1986

Prepared for the Division of Engineering Technology
Office of Nuclear Regulatory Research
U. S. Nuclear Regulatory Commission
Washington, D. C. 20555

NRC FIN No. A2243

LONG-TERM EMBRITTLEMENT OF CAST-DUPLEX STAINLESS STEELS
IN LWR SYSTEMS:

ANNUAL REPORT
October 1984--September 1985


ABSTRACT

This progress report summarizes work performed by Argonne National Laboratory on long-term embrittlement of cast duplex stainless steels in LWR systems during the 12 months from October 1984 to September 1985.


| NRC FIN No. | FIN Title |
|---|---|
| A2243 | Long-Term Embrittlement of Cast Duplex Stainless Steels in LWR Systems |

Previous Annual Reports in this Series

| | |
|---|---|
| NUREG/CR-3857, ANL-84-44 | October 1982-September 1983 |
| NUREG/CR-4204, ANL-85-20 | October 1983-September 1984 |

TABLE OF CONTENTS

LONG-TERM EMBRITTLEMENT OF CAST-DUPLEX STAINLESS STEELS
IN LWR SYSTEMS:

ANNUAL REPORT[a]
October 1984--September 1985

## EXECUTIVE SUMMARY

A program is being conducted to investigate the significance of in-service embrittlement of cast-duplex stainless steels under light-water reactor operating conditions. Data from room-temperature Charpy-impact tests for several heats of cast stainless steel aged up to 10,000 h at 290, 320, 350, 400, and 450°C are presented and compared with results from other studies. Microstructures of cast-duplex stainless steels subjected to long-term aging up to eight years either in the laboratory or in reactor service have been characterized. The results indicate that at least two processes contribute to the low-temperature embrittlement of duplex stainless steels, viz., weakening of the ferrite/austenite phase boundary by carbide precipitation and embrittlement of ferrite matrix by the formation of additional phases such as G-phase, Type X, or the α' phase. Carbide precipitation has a significant effect on the onset of embrittlement of CF-8 and -8M grades of stainless steels aged at 400 or 450°C. The existing correlations do not accurately represent the embrittlement behavior over the temperature range 300 to 450°C.

[a]NRC FIN Budget No. A2243; NRC Contact: J. Muscara.

# LONG-TERM EMBRITTLEMENT OF CAST DUPLEX STAINLESS STEELS IN LWR SYSTEMS:

ANNUAL REPORT
October 1984-September 1985

Principal Investigators:
O. K. Chopra and H. M. Chung

## I. INTRODUCTION

The primary objectives of this program are: (1) to investigate the significance of in-service embrittlement of cast-duplex stainless steels under light-water reactor (LWR) operating conditions, and (2) to evaluate possible remedies to the embrittlement problem for existing and future plants.

The scope includes the following: (1) characterize and correlate the microstructure of in-service reactor components and laboratory-aged material with loss of fracture toughness and identify the mechanism of embrittlement, (2) determine the validity of laboratory-induced embrittlement data for predicting the toughness of component materials after long-term aging at reactor operating temperatures, (3) characterize the loss of fracture toughness in terms of fracture mechanics parameters in order to provide the data needed to assess the safety significance of embrittlement, and (4) provide additional understanding of the effects of key compositional and metallurgical variables on the kinetics and degree of embrittlement. The relationship between aging time and temperature for onset of embrittlement will be determined by microstructural examination and measurements of hardness, Charpy-impact strength, tensile strength, and $J_{IC}$ fracture toughness. The kinetics and fracture toughness data generated in this program and from other sources will provide the technical basis for assessing the in-service embrittlement of cast stainless steels under LWR operating conditions. Estimates of the degree of embrittlement will be compared with data obtained from examination of material from actual reactor service. Data pertaining to the effects of compositional and metallurgical variables on the embrittlement phenomenon will help in evaluation of the possible remedies for in-service embrittlement of components in existing and future plants.

## II. SUMMARY OF RESEARCH PROGRESS

The main areas of effort during the past year have been (a) material characterization, (b) mechanical properties of short- and medium-term aged material, and (c) characterization of the microstructure and fracture morphology of reactor aged and long-term laboratory aged material.

### A. Material Characterization

Material was obtained from nineteen experimental heats (static-cast keel blocks) and six commercial heats (centrifugally cast pipes and static-cast pump impeller and pump casing ring) of CF-3, -8, and -8M grades of cast-duplex stainless steel. Six of the experimental heats were also procured in the form of 76-mm-thick slabs. Charpy-impact specimen blanks were obtained from all heats of material. Blanks for compact tension and tensile specimens were obtained from sections of cast pipes, pump casing ring, pump impeller, and the cast slabs. The specimen blanks are being aged at 450, 400, 350, 320, and 290°C for times up to 50,000 h. Materials from the reactor components and small experimental heats have completed ~11,000 h of aging and cast materials from the large experimental heats (76-mm-thick slabs) have completed ~4000 h of aging. The mechanical test specimens are machined after the thermal aging treatment.

Fractured impact test bars from three heats of aged cast stainless steel, grades CF-8 and CF-8M, were obtained from Georg Fischer Co., Switzerland, for microstructural characterization. The materials are from a previous study of the long-term aging behavior of cast stainless steel.[1] The specimens from CF-8 material (Heats 280 and 278) were aged for 3000, 10,000, and 70,000 h at 300, 350, and 400°C, whereas the specimens from CF-8M material (Heat 286) were aged for 1000 and 10,000 h at 400°C. A cover plate assembly from the recirculation pump of the KRB reactor was also procured. The reactor was in service for ~12 yr. The plate assembly was decontaminated and samples were obtained for microstructural characterization and mechanical testing. The test matrices for the various mechanical tests and microstructural examination have been presented.[2,3]

Data on the chemical composition, ferrite content, hardness, ferrite morphology, and grain structure of the small experimental and commercial heats have been reported.[4-6] The centrifugally cast pipe material contains equiaxed or radially oriented columnar grains, while the static-cast keel blocks, slabs, and the pump impeller contain a mixed grain structure. The ferrite contents of the cast materials range between 3 and 30%. The ferrite morphology for the castings containing >5% ferrite is either lacy or acicular. A change in the ferrite content of the duplex material has very little effect on the concentrations of Ni and Cr in the two phases. For all materials, some differences in the chemical composition, ferrite content, and hardness are observed for material from the top or bottom region of the static-cast keel blocks and slabs or the inner and outer diameter of the centrifugally cast pipes. In general, the hardness of the cast material increases with an increase in ferrite content. For the same ferrite content, the hardness of CF-8 and -8M material is comparable, while the hardness of CF-3 material is lower. An increase in nitrogen content increases the hardness of all grades of cast stainless steel.

Characterization of the six large experimental heats has also been completed. The heats were static cast in the form of square slabs (0.61 x 0.61 m) 76-mm thick. All materials were examined in the three orientations as well as in different locations, namely, material from the top, middle, and bottom section of the slabs. Orientation of the material had little or no effect on either hardness or ferrite content and morphology. The chemical composition, hardness, and ferrite content of the different heats are given in Table 1. Small experimental heats (i.e., keel blocks) with chemical composition and ferrite contents equivalent to the large experimental heats are also listed in Table 1. The hardness and ferrite content values represent the average values for the three locations.

The grain structures of the large experimental heats are shown in Fig. 1. All heats contain a mixed structure of columnar and equiaxed grains. A change from horizontal to vertical growth of the columnar grains was observed near the edges of the cast slabs, e.g., Heat 73. The grain size of Heats 69 (grade CF-3) and 75 (grade CF-8M) is smaller than that for the other heats.

Table 1. Chemical Composition and Ferrite Content of Cast Stainless Steel

| Heat | Grade | Composition, wt % | | | | | | | Hardness $R_B$ | Ferrite Content, % | |
|---|---|---|---|---|---|---|---|---|---|---|---|
| | | Mn | Si | Mo | Cr | Ni | N | C | | Calc.[a] | Meas.[b] |
| | | | | | Cast Slabs[c] | | | | | | |
| 73 | CF-8 | 0.83 | 1.22 | - | 19.53 | 8.94 | 0.05 | 0.06 | 78.8 | 7.4 | 7.7 |
| 68 | CF-8 | 0.67 | 1.13 | - | 20.85 | 8.08 | 0.06 | 0.05 | 84.6 | 18.8 | 23.4 |
| 74 | CF-8 | 0.77 | 1.21 | - | 20.73 | 8.17 | 0.11 | 0.06 | 85.8 | 10.5 | 18.4 |
| 69 | CF-3 | 0.69 | 1.20 | - | 20.49 | 8.43 | 0.03 | 0.02 | 83.7 | 25.7 | 23.6 |
| 70 | CF-8M | 0.70 | 0.74 | 2.64 | 19.37 | 9.13 | 0.05 | 0.07 | 86.5 | 15.8 | 18.9 |
| 75 | CF-8M | 0.59 | 0.67 | 2.40 | 21.07 | 9.02 | 0.05 | 0.06 | 89.5 | 27.1 | 27.8 |
| | | | | | Keel Blocks[d] | | | | | | |
| 56 | CF-8 | 0.60 | 1.16 | 0.30 | 19.33 | 8.93 | 0.03 | 0.06 | 82.5 | 8.1 | 10.1 |
| 60 | CF-8 | 0.71 | 1.01 | 0.26 | 21.02 | 8.07 | 0.05 | 0.07 | 86.7 | 16.9 | 21.1 |
| 51 | CF-3 | 0.66 | 1.06 | 0.28 | 20.36 | 8.69 | 0.05 | 0.02 | 83.8 | 17.5 | 18.0 |
| 66 | CF-8M | 0.71 | 0.60 | 2.36 | 19.41 | 9.13 | 0.03 | 0.06 | 85.2 | 17.9 | 19.9 |
| 64 | CF-8M | 0.70 | 0.71 | 2.41 | 20.87 | 9.01 | 0.03 | 0.05 | 89.7 | 32.2 | 28.4 |

[a]Calculated from the chemical composition with Hull's equivalent factor.
[b]Measured by ferrite scope Auto Test FE, Probe Type FSP-1).
[c]Chemical compositions obtained from the vendor.
[d]Chemical compositions obtained at Argonne National Laboratory.

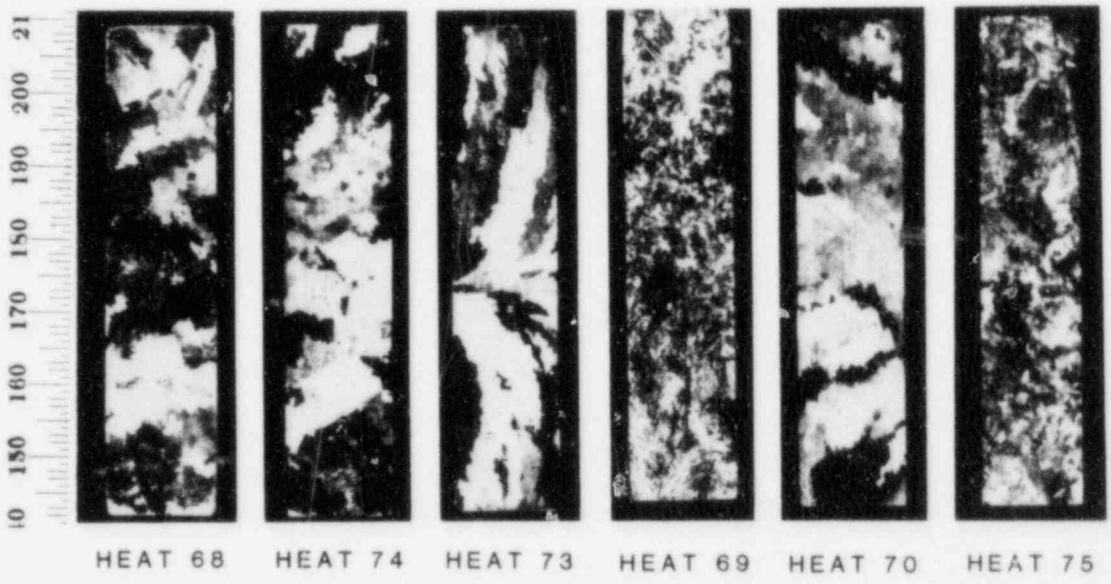


Fig. 1. Microstructures Along the Vertical Sections of the Various Static Cast Slabs.

The ferrite morphologies for the large experimental heats are shown in Figs. 2-4. The CF-8 and -8M grades of cast stainless steels have a lacy morphology, i.e., an interlaced network of ferrite islands. The CF-3 grade of cast steel has a mixture of lacy and acicular morphology. The acicular morphology is characterized by fine needle-like ferrite distributed in the austenite matrix. The ferrite contents and morphologies for the large experimental heats are similar to those observed for the corresponding heats of the keel blocks.

## B. Mechanical Properties of Aged Material

Charpy-impact tests are in progress at room temperature on the various heats of material aged up to 10,000 h at 450, 400, 350, 320, and 290°C. Standard Charpy V-notch specimens were machined from the aged and unaged materials according to ASTM specification E-23. A Dynatup Model 8000A drop-weight impact machine with an instrumented tup and data-readout system was used for the tests. Charpy-impact energies for materials aged for 3000 h at 450, 400, 350, 320°C, and 290°C are given in Table 2. The results indicate that thermal aging of cast-duplex stainless steels with >10% ferrite causes a substantial decrease in impact energy. Materials with >20% ferrite show a drastic reduction in impact energy after aging for ~300 h at 450°C or ~3000 h at 400°C. In general, the low-carbon grades of cast stainless steels exhibit greater resistance to embrittlement than the CF-8 and -8M grades.

Figure 5 shows the load-time curves for Heat 60 in the unaged condition and after aging for 300, 3000, and 10,000 h at 400°C. The results show two important features, namely, thermal aging leads to a reduction in impact energy and an increase in the strain hardening rate of the material. The strain hardening rate increases after aging for a relatively short time (i.e., ~300 h) and does not change significantly with further aging. The maximum load for a specimen that was aged for 300 h is greater than that for the unaged material. The higher strain hardening rates for the aged material are associated with the precipitation reactions in the ferrite matrix. The load-time curve for a specimen that was aged for 10,000 h exhibits a sudden drop in load, indicating a brittle fracture mode. Such load-time curves were typical of all heats containing >20% ferrite.

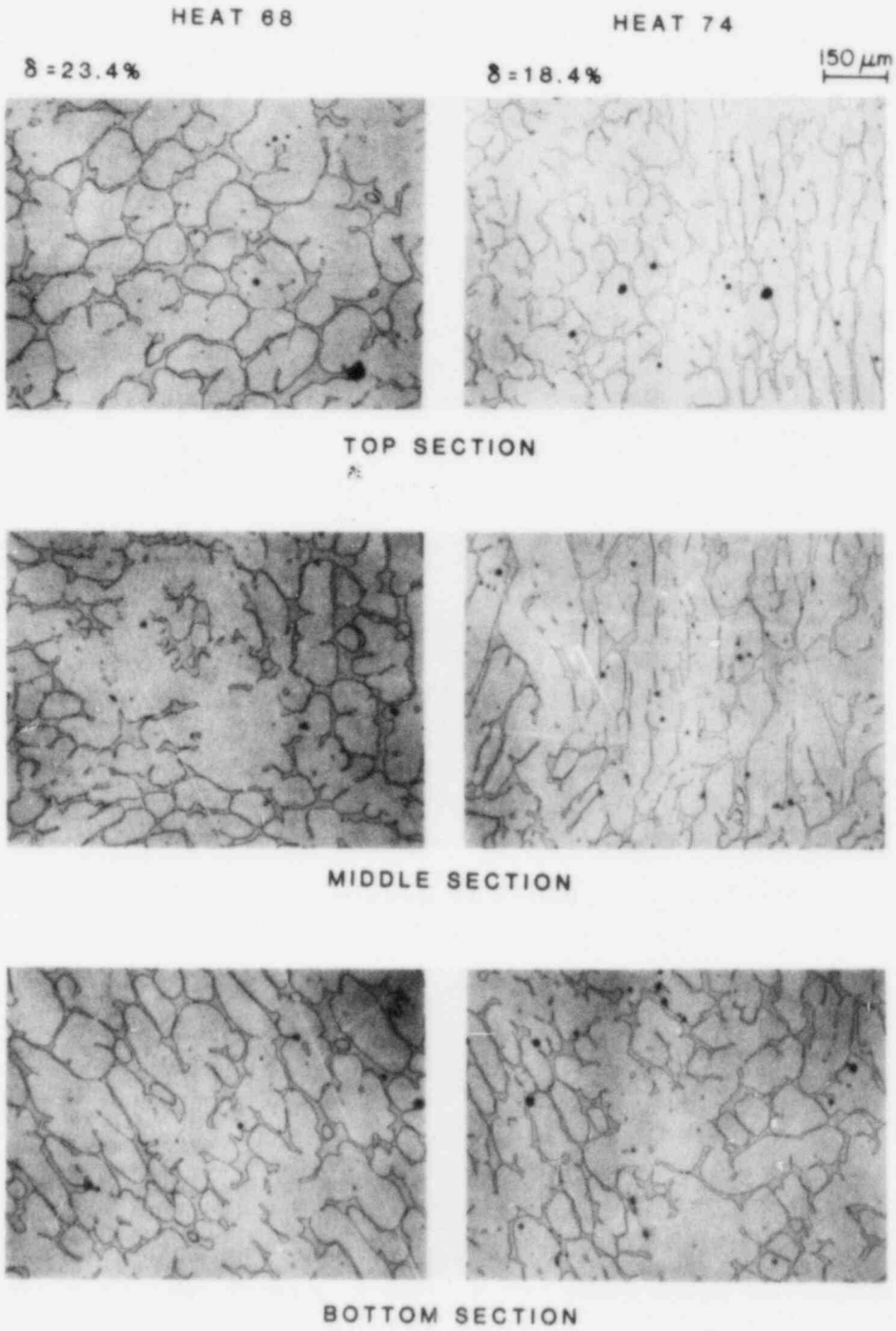


Fig. 2. Microstructures from Three Locations of the Static Cast Slabs of CF-8 Stainless Steel.

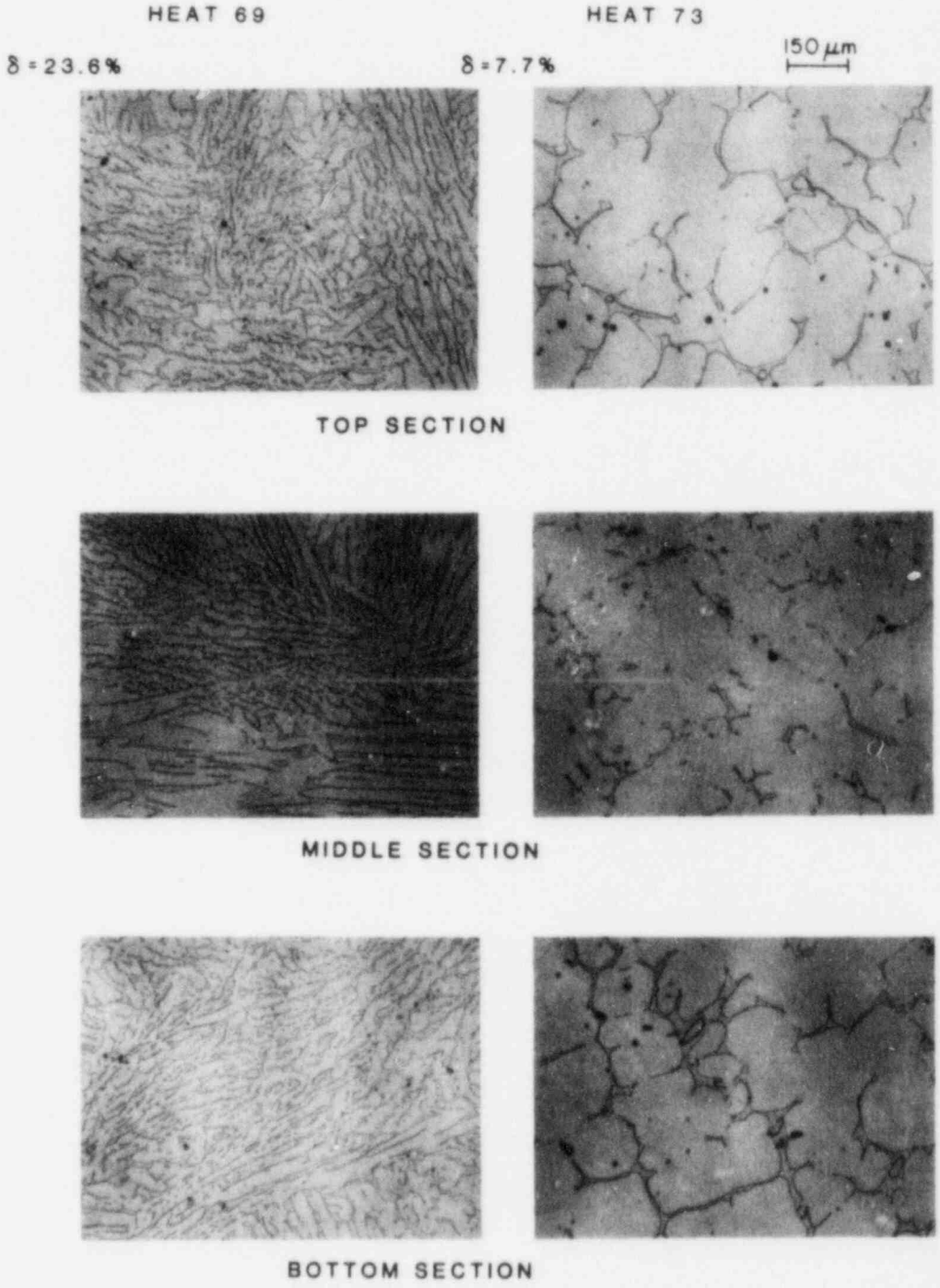


Fig. 3. Microstructures from Three Locations of the Static Cast Slabs of CF-3 (Heat 69) and CF-8 (Heat 73) Stainless Steel.

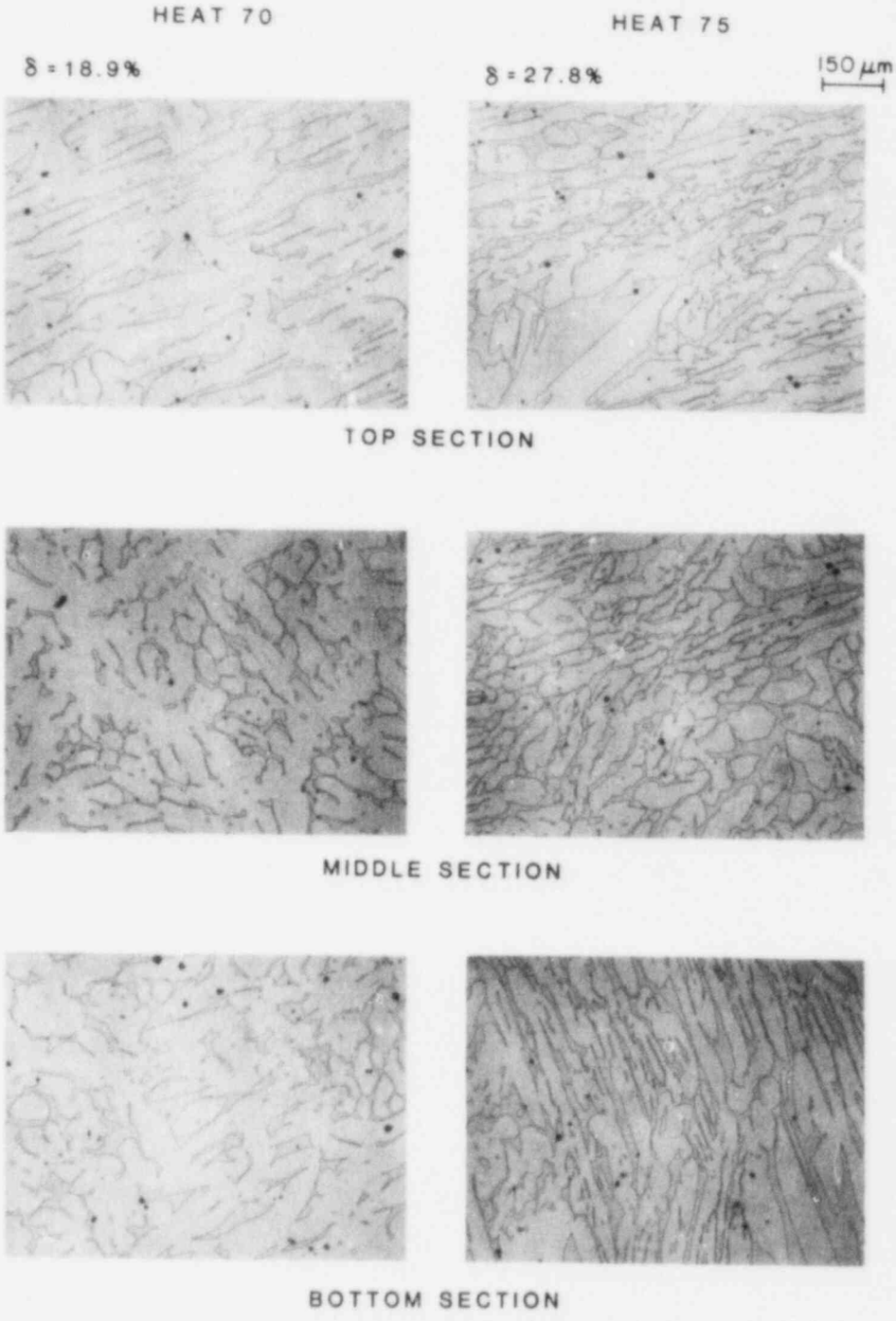


Fig. 4. Microstructures from Three Locations of the Static Cast Slabs of CF-8M Stainless Steel.

Table 2. Charpy-Impact Data Obtained at Room Temperature for Thermally Aged Cast Stainless Steel

| Heat | Ferrite Content, % | Impact Energy,[a] J | | | | | |
|---|---|---|---|---|---|---|---|
| | | | Aged for 3000 h at | | | | |
| | | Unaged | 290°C | 320°C | 350°C | 400°C | 450°C |
| | | | CF-8 | | | | |
| 56 | 10.1 | 165 | 147 | 151 | 146 | 134 | 105 |
| 59 | 13.5 | 183 | 147 | 161 | 135 | 132 | 95 |
| 61 | 13.1 | 201 | 149 | 155 | 152 | 148 | 100 |
| 60 | 21.1 | 158 | 135 | 150 | 149 | 64 | 51 |
| C1 | 2.2 | 47 | - | - | 41 | 46 | 48 |
| P1 | 24.1 | 178 | 208 | 170 | 158 | 45 | 53 |
| | | | CF-3 | | | | |
| 52 | 13.5 | 198 | 149 | 175 | 189 | 174 | 146 |
| 47 | 16.3 | 184 | 172 | 245 | 179 | 151 | 140 |
| 51 | 18.0 | 161 | 150 | 143 | 164 | 131 | 125 |
| P3 | 1.9 | 241 | - | 273 | 225 | 292 | 312 |
| P2 | 15.6 | 321 | 362 | 357 | - | 212 | 158 |
| I | 17.1 | 156 | - | 152 | 156 | - | 105 |
| | | | CF-8M | | | | |
| 63 | 10.4 | 199 | - | 137 | 166 | 125 | 126 |
| 66 | 19.9 | 177 | 149 | 204 | 166 | 113 | 84 |
| 65 | 23.4 | 179 | 154 | 147 | 141 | 51 | 51 |
| 64 | 28.4 | 160 | - | 140 | 120 | 40 | 42 |
| P4 | 10.4 | 182 | 175 | 198 | 108 | 74 | 36 |

[a]Tests performed on instrumented drop-weight impact machine with V-notch impact bars (ASTM specification E-23).

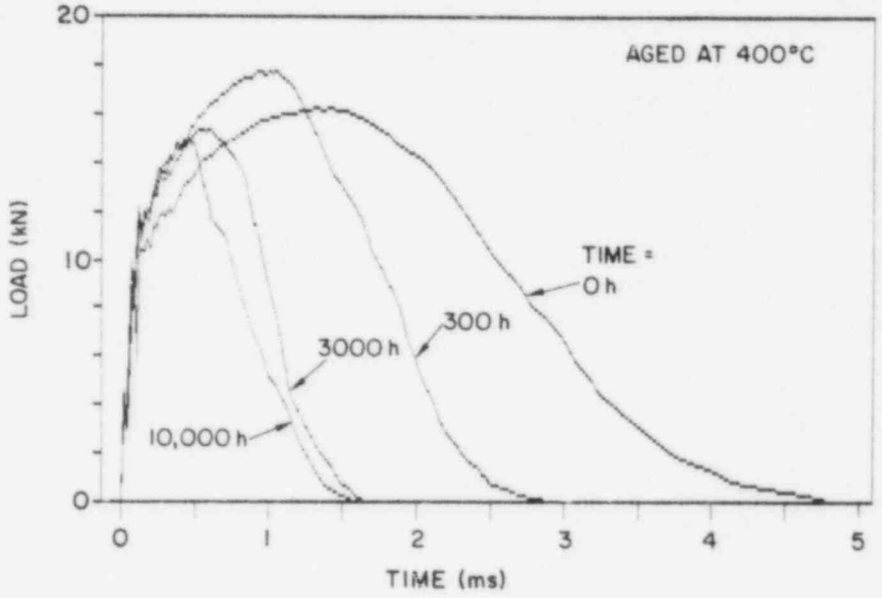


Fig. 5. Load-Time Curves for Charpy V-notch Specimens of Heat 60 Tested at Room Temperature.

The Charpy-impact data for some of the heats of cast stainless steel are presented in Figs. 6-9 and compared with the results from studies by Georg Fischer Co., Switzerland (GF)[1] and Framatome, France (FRA).[7] The chemical composition and the ferrite content of the various materials are given in Table 3. The different temperatures and times for aging were normalized in terms of the parameter P, which is determined from

$$t = 10^{P} \exp\left[\frac{Q}{R}\left(\frac{1}{T} - \frac{1}{673}\right)\right], \qquad (1)$$

where Q is the activation energy, R the gas constant, T the absolute temperature, and P the aging parameter which represents the degree of aging reached after $10^{P}$ h at 400°C. The activation energy for the process of embrittlement has been described as a function of chemical composition of the cast material.[7] Thus,

$$Q(\text{kcal/mole}) = -43.64 + 4.76\ (\%\ \text{Si}) + 2.65\ (\%\ \text{Cr}) + 3.44\ (\%\ \text{Mo}). \qquad (2)$$

The service time at 320°C is also shown in each figure. The significant results are as follows.

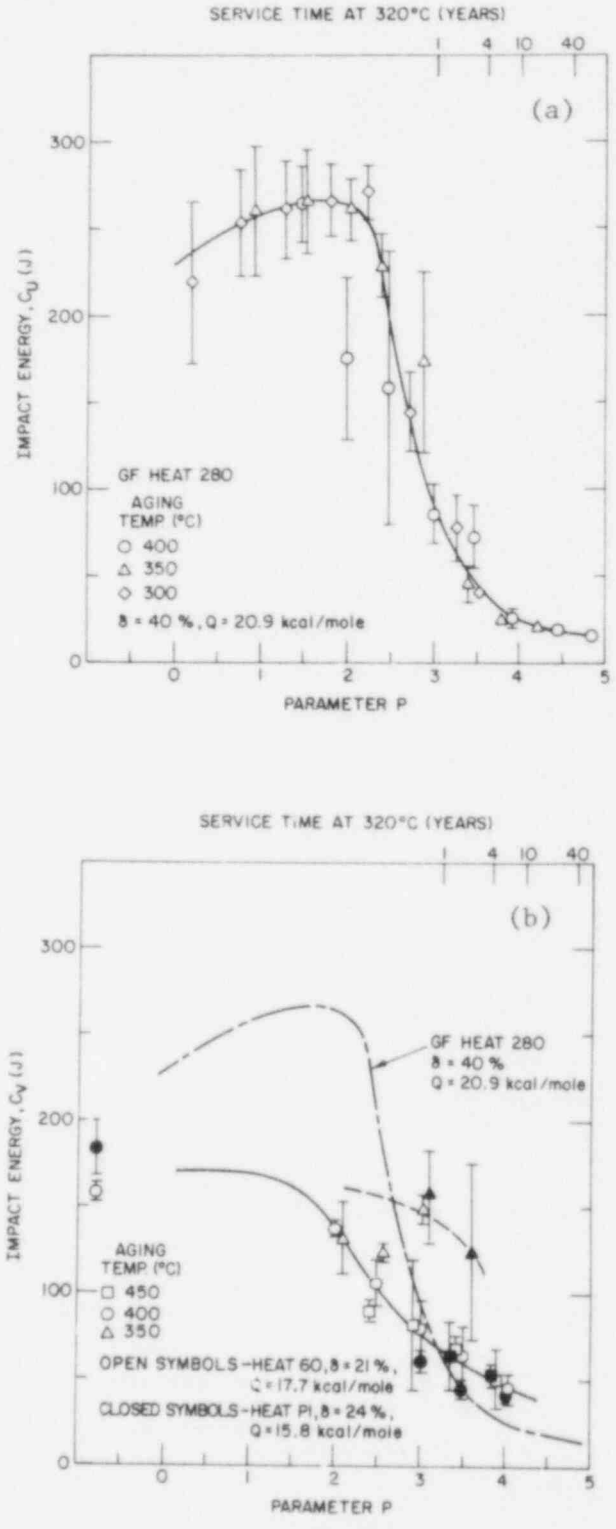


Fig. 6. Influence of Thermal Aging on the Room-Temperature Impact Energy of CF-8 and -3 Cast Stainless Steel. (a) Georg Fischer (GF) Heat 280 (Ref. 1) and (b) Heats 60 and P1.

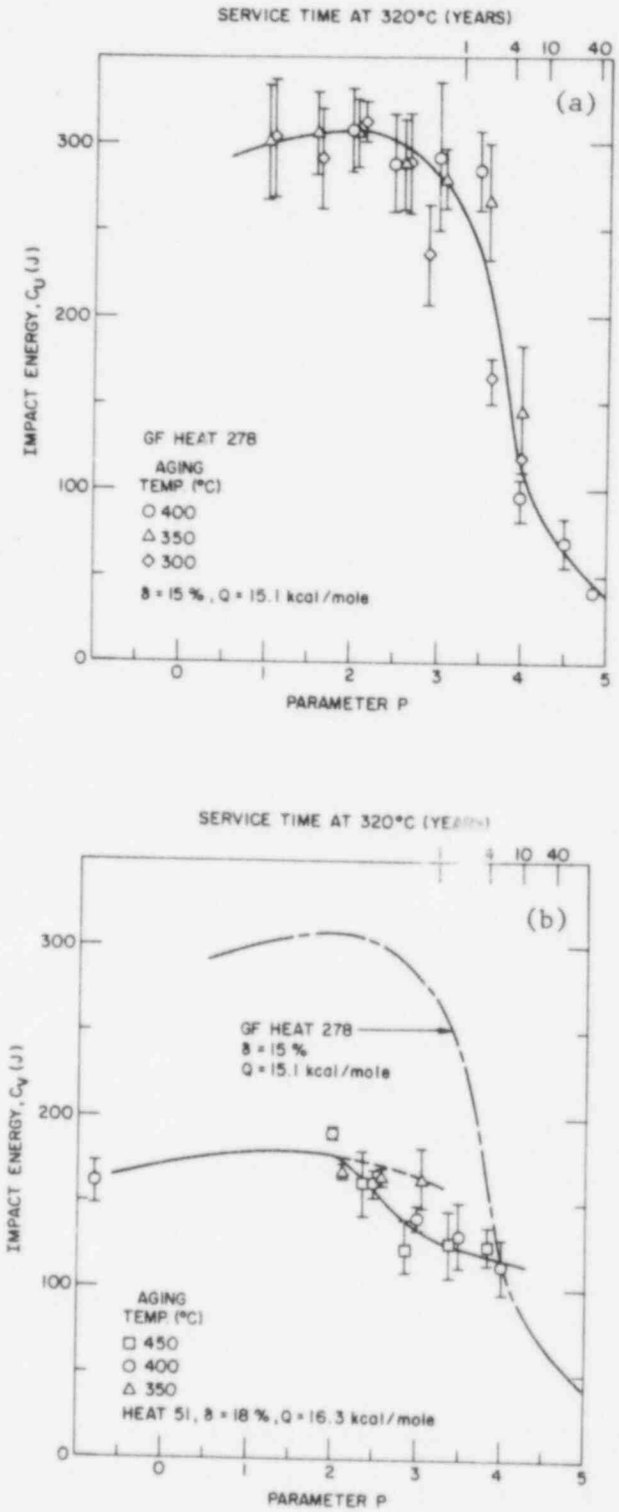


Fig. 7. Influence of Thermal Aging on the Room-Temperature Impact Energy of CF-8 and -3 Cast Stainless Steel. (a) Georg Fischer (GF) Heat 278 (Ref. 1) and (b) Heat 51.

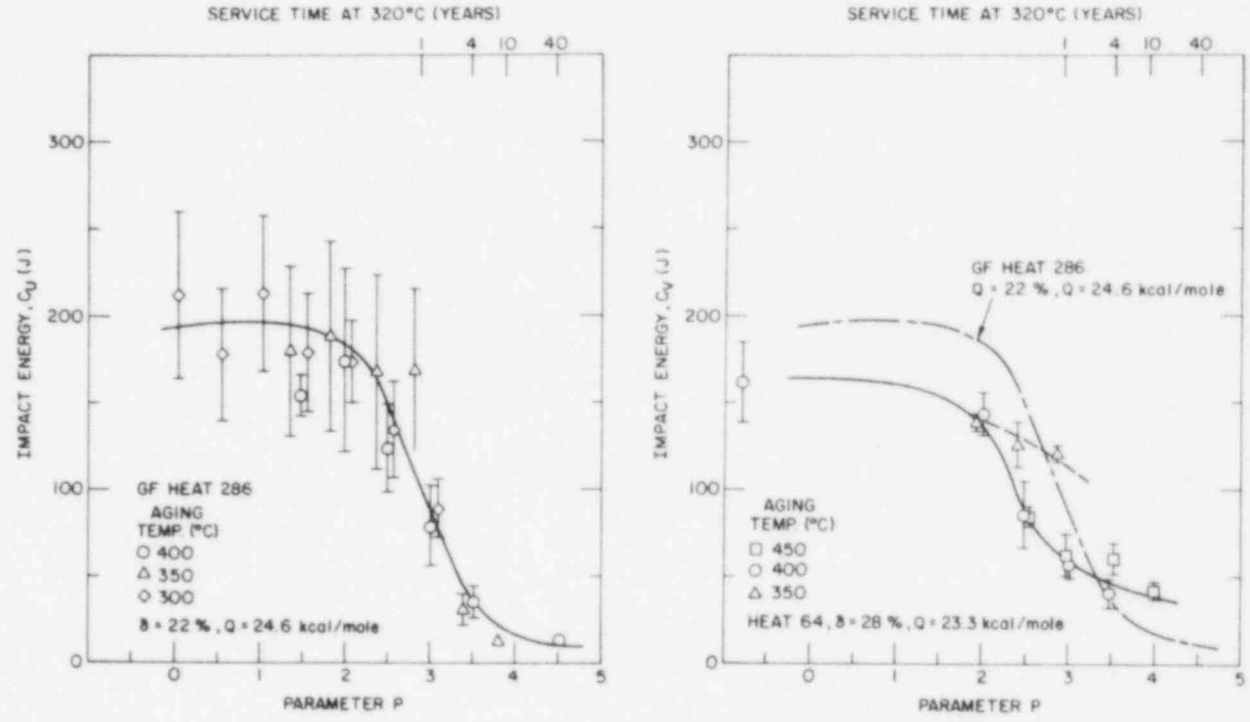


Fig. 8. Influence of Thermal Aging on the Room-Temperature Impact Energy of CF-8M Cast Stainless Steel. (a) Georg Fischer (GF) Heat 286 (Ref. 1) and (b) Heat 64.

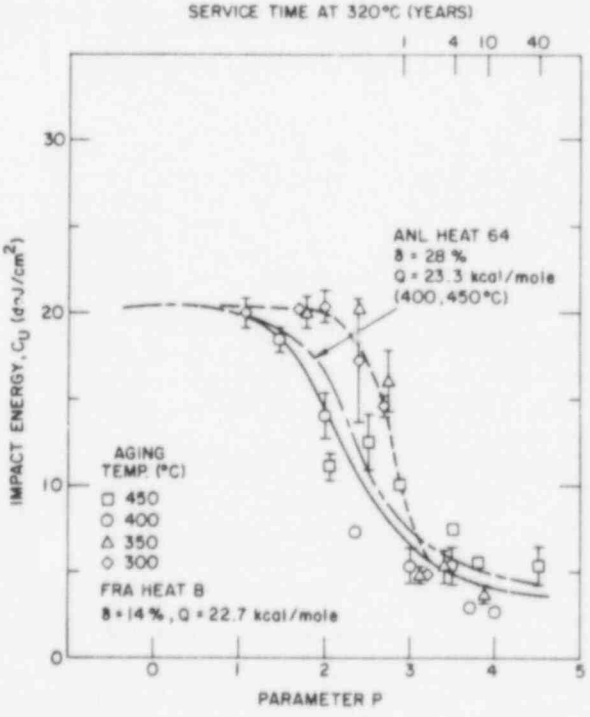


Fig. 9.
Influence of Thermal Aging on the Normalized Impact Energy at Room Temperature for CF-8 Cast Stainless Steel (Ref. 7).

Table 3. Chemical Composition and Ferrite Content of Cast Stainless Steel

| Heat | Chemical Composition, wt % | | | | | | | Ferrite Content, % | |
|---|---|---|---|---|---|---|---|---|---|
| | Si | Mn | Ni | Cr | Mo | C | N | Calculated[a] | Measured[b] |
| **Experimental Heats** | | | | | | | | | |
| 60 | 1.01 | 0.71 | 8.07 | 21.02 | 0.26 | 0.070 | 0.050 | 16.9 | 21 |
| 51 | 1.06 | 0.66 | 8.69 | 20.36 | 0.28 | 0.023 | 0.048 | 17.5 | 18 |
| 64 | 0.71 | 0.70 | 9.01 | 20.87 | 2.41 | 0.050 | 0.030 | 32.2 | 28 |
| **Commercial Heat** | | | | | | | | | |
| P1 | 1.07 | 0.56 | 8.10 | 20.49 | 0.04 | 0.032 | 0.053 | 18.8 | 24 |
| **Pump Cover Plate from KRB Reactor[c]** | | | | | | | | | |
| KRB | 1.17 | 0.31 | 8.03 | 21.99 | 0.17 | 0.062 | 0.038 | 27.7 | 26 |
| **Georg Fischer Heats[d]** | | | | | | | | | |
| 280 | 1.37 | 0.50 | 8.00 | 21.60 | 0.25 | 0.028 | 0.029 | 38.6 | 40 |
| 278 | 1.00 | 0.28 | 8.27 | 20.20 | 0.13 | 0.038 | 0.027 | 19.0 | 15 |
| 286 | 1.33 | 0.40 | 9.13 | 20.20 | 2.44 | 0.072 | 0.063 | 18.7 | 22 |
| **Framatome Heat[e]** | | | | | | | | | |
| B | 0.93 | 0.83 | 10.56 | 20.12 | 2.52 | 0.053 | 0.042 | 14.0 | - |

[a]Calculated from chemical composition with Hull's equivalent factor.
[b]Measured by ferrite scope (Auto test FE, Probe Type FSP-1).
[c]The material was in service for ~12 yr at 284°C. A 75% capacity factor is assumed.
[d]Fractured Charpy-impact bars were obtained from Georg Fischer Co., Switzerland, for microstructural evaluation. Charpy-impact test data from Ref. 1.
[e]Charpy-impact test data from Ref. 7.

(a) The time-temperature correlations given in Eqs. (1) and (2) are valid for each of the three GF heats of material, i.e., the data for aging temperatures of 300, 350, and 400°C can be represented by a single correlation between impact energy and parameter P. The impact energy for Heat 286 aged at 400°C for relatively short times (i.e., P <2.5) is slightly lower than that for the material aged at 350 or 300°C, Fig. 8a. Table 3 shows that the carbon content in Heat 286 is significantly higher than in Heats 280 or 278. The results also indicate that the time for the onset of embrittlement is different for the different materials, e.g., ~2 yr service at 320°C for Heat 278 and <1 yr service at 320°C for Heats 280 and 286.

(b) The data for the materials used in the present investigation and for FRA Heat B do not follow a single curve. The impact energy for the materials aged at 450 and 400°C decreases much more rapidly than for the materials aged at 350 or 300°C, i.e., the onset of embrittlement is sooner for materials aged at 450 and 400°C than for those aged at lower temperatures. The difference between high- and low-temperature data is greater for Heats 60, P1, 64, and B containing >0.05 wt % C relative to Heat 51 with ~0.02 wt % C. Results for FRA Heat B indicate that the impact energies are comparable for material aged at high or low temperatures for long times, Fig. 9.

(c) The impact energies of the unaged GF heats are significantly higher than those for the other heats. This difference may be attributed to the unique heat treatment of the materials. The GF heats were reheat-treated in the laboratory after the commercial heat treatment, while the other heats were in the commercial heat-treated condition. The room-temperature impact energies of the unaged GF heats probably correspond to the upper shelf energy, whereas the values for the other heats represent the ductile-to-brittle transition.

(d) After 10,000 h aging at 400°C, the low-carbon Heat 51 shows a relatively small reduction in impact energy compared to other heats with higher carbon but a comparable ferrite content. For example, the impact energy decreases by ~30% for Heat 51 containing 18% ferrite, whereas Heat 60 with 21% ferrite and GF Heat 278 with 15% ferrite show a reduction in impact strength of >70%.

The change in impact energy of cast CF-8 stainless steel after reactor service is shown in Fig. 10. The specimens were obtained from the KRB pump cover plate which was in service for ~12 yr at a nominal temperature of 284°C. The actual temperature of the test material ranged between 265 and 278°C. The impact energies of the KRB material are slightly higher than those predicted by the average curve for GF Heat 280 or the Argonne Heat 60.

These results indicate that the activation energies obtained from Eq. (2) do not accurately represent the embrittlement behavior of cast stainless steels over the entire temperature range of 300 to 450°C. The carbon content in the steel appears to play an important role in the overall process of embrittlement. The rapid decrease in impact energy during high-temperature aging, i.e., at 400 and 450°C, is most likely caused by the precipitation of carbides in the ferrite matrix or at the ferrite/austenite boundary. Such processes either do not occur or are too slow at lower temperatures, and the embrittlement of the steel is primarily caused by the formation of other phases, such as $\alpha'$ or G phase.

Figure 11 shows the influence of thermal aging on the impact energy and microhardness of the ferrite phase for Heat 51 (grade CF-3) and Heat 60 (grade CF-8). The results indicate that the impact energy decreases and the microhardness of the ferrite phase increases with aging time. For a given aging condition, the microhardness of the ferrite is comparable for Heats 51 and 60. However, the reduction in impact energy is significantly higher for Heat 60 than for Heat 51. Microstructural characteristics of Heats 51 and 60, discussed in the next section, suggest that the difference in impact strength arises from the precipitation of carbides at the ferrite/austenite phase boundaries in Heat 60.

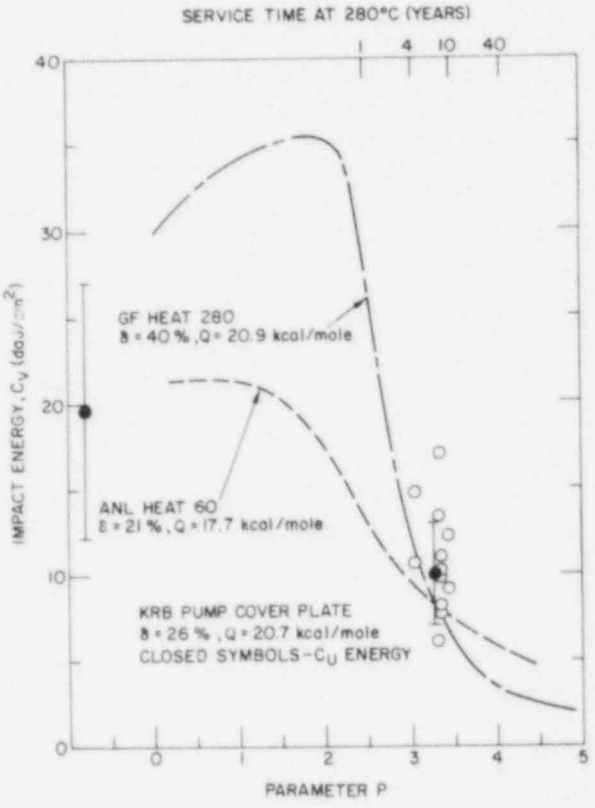


Fig. 10. Normalized Impact Energy at Room Temperature for CF-8 Cast Stainless Steel after ~12-yr Service at ~284°C.

Materials from two centrifugally cast pipes and a static cast pump impeller, aged up to 10,000 h at 400 and 350°C, were sent to Materials Engineering Associates (MEA), Washington, for J-R curve determination and tensile tests. Tensile specimens (with a 5.1-mm diameter and an 18.5-mm gauge length) and 1-T compact tension specimens were fabricated from the aged materials. Mechanical tests are in progress at room temperature and at 290°C.

## C. Microstructural Characterization

Microstructures of the aged and fractured impact test specimens were characterized by TEM, SEM, optical microscopy, and small-angle neutron scattering (SANS) techniques. The results of a microstructural examination of the GF materials and the KRB pump cover plate have been reported previously,[2,5,6,8] The microstructural characteristics were correlated with the fracture behavior of the impact specimens to provide a better understanding of the embrittling mechanism(s) of cast-duplex stainless steels.[8] The results showed that three phases were responsible for the embrittlement of the ferrite

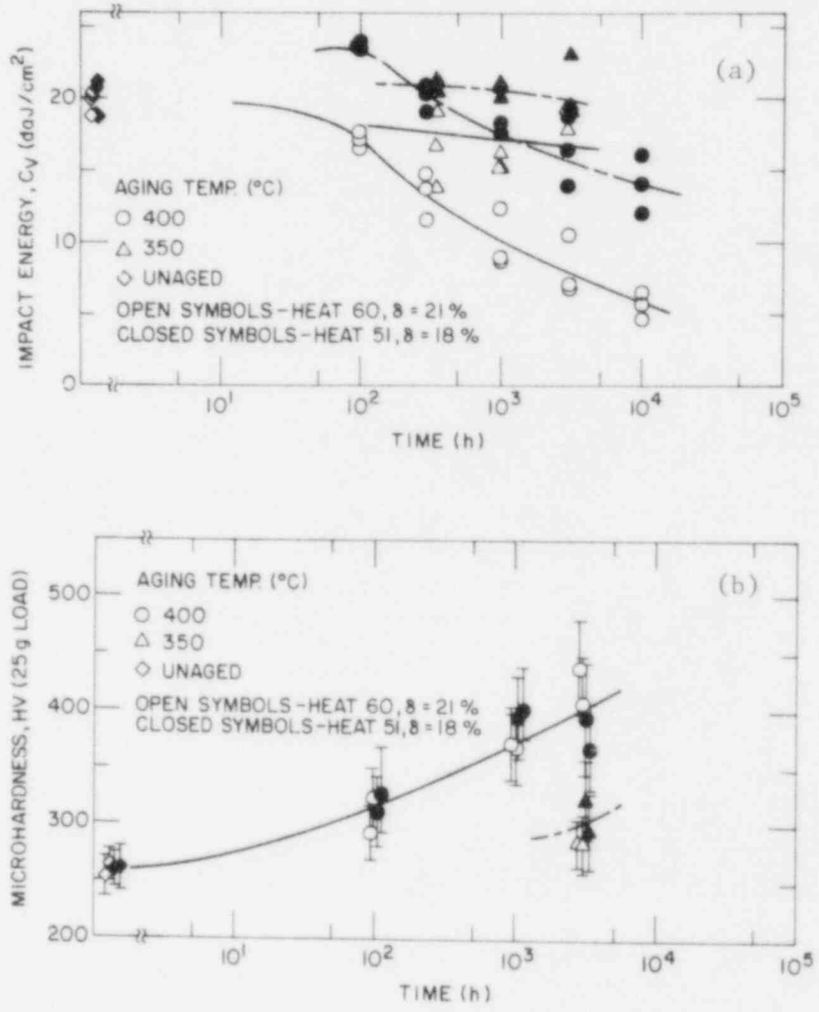


Fig. 11. Influence of Thermal Aging on the (a) Room-Temperature Impact Energy and (b) Microhardness of the Ferrite Phase for CF-3 (Heat 51) and CF-8 (Heat 60) Grades of Cast Stainless Steel.

phase. Precipitation on the ferrite/austenite phase boundary was also identified and was found to be responsible for the weakening of the phase boundary.

1. Embrittlement of the Ferrite Phase

The characteristics of the three precipitates, i.e., G-phase, Type X, and the chromium-rich α', can be summarized as follows:

G-Phase. Figure 12 shows the characteristic morphology and selected-area diffraction (SAD) patterns of the G-phase observed in the GF material after aging at 400°C for 7.6 yr. The precipitates were also observed

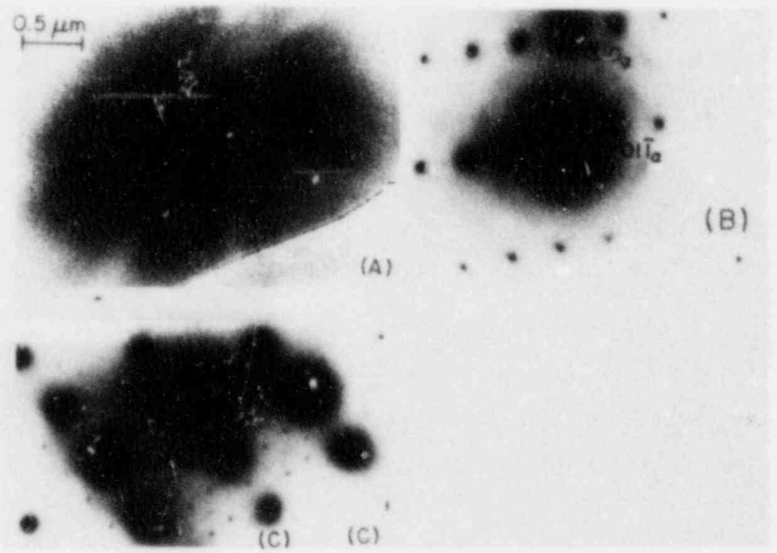


Fig. 12. Dark-Field Morphology (A) and Characteristic SAD Patterns (B and C) of the Ni- and Si-rich G-Phase Observed in CF-8 Cast-Duplex Stainless Steel after Aging at 400°C for 7.6 yr.

in the reactor-aged pump cover material, which was exposed to the coolant at ~274°C for ~12 yr. Volume fractions of the G-phase in the KRB pump material or in GF Heats 280 and 278, aged at 300°C for ~8 yr (Figs. 6 and 7), were not large enough to produce distinct reflections in the diffraction patterns [similar to those of Figs. 12(B) and (C)]. Although 400°C aging produced precipitates of the G-phase in the ferrite grains as well as on the grain boundaries [Fig. 12(A)], no grain boundary precipitation was observed after aging at $\lesssim$300°C. During lower temperature aging, the precipitates were observed primarily in association with dislocations in the ferrite; this observation indicates a dislocation pinning effect. The nearly spherical precipitate is ~5 nm in size. The diffraction patterns are similar to those of the $M_{23}C_6$ phase, but with a slightly larger lattice parameter. The precipitates also had a cube-on-cube orientation relative to the bcc ferrite matrix, which would be unusual for the $M_{23}C_6$ phase. (400) reflections were characteristically weak or absent in the diffraction patterns [Fig. 12(C)]. Energy-dispersive x-ray analysis showed an enrichment of Ni and Si in the precipitates. From these results, the precipitates were identified as the G-phase (a phase rich in Ni and Si), which has been observed in an Fe-12Cr-4Ni

alloy after aging at 450°C[9] and in commercial EM-12 (9Cr-2Mo), HT-9 (12Cr-1Mo), and AISI 416 (13Cr) ferritic steels after irradiation at temperatures of <425°C.[10] The G-phase has also been identified by atom probe field-ion microscopy in cast duplex stainless steel aged for 7500 h at 400°C.[11,12]

Type X Precipitates. In both the KRB pump material and GF Heats 280 and 278, aged at 300°C for 8 yr, the unidentified (Type X) precipitate was always observed on dislocations. Figure 13 shows the morphology of the precipitates observed in the KRB pump material that are interwoven with the dislocations. Apparently, the precipitates were very effective in pinning dislocation motion in the material aged for a long time near 300°C. The precipitate reflections in the SAD patterns were weak, diffuse, and streaked, owing to a low volume fraction and small particle size. In typical SAD patterns containing the Type-X precipitates, only extremely weak precipitate reflections with a d-spacing of 0.218 nm were detected. The weak reflections could not be detected on the microscope screen. No cross-grid patterns could be obtained.

α' Precipitate. Chromium-rich α' precipitates in the ferrite were observed in KRB pump-cover material, Fig. 14(A). The extremely small (1-2 nm) α' precipitates could not be resolved by TEM either under a strong bright-field or dark-field imaging condition. The precipitates could be resolved only under a weak-beam imaging condition. The mottled morphology characteristic of the α' was difficult to resolve in the GF material after aging at 300°C for 8 yr. However, optimum weak-beam imaging[13] at a magnification of 20-40 thousand times revealed α' precipitates 1-1.5 nm in size when the negatives were developed and examined on a lighted table with a magnifying glass. Negatives taken under normal bright- or dark-field imaging condition did not reveal any α' precipitates in the GF materials. Figure 14(B) shows the α' in the ferrite of Heat 60 after aging at 400°C for 1.2 yr. The α' size and morphology are similar to those of the KRB reactor-aged material.

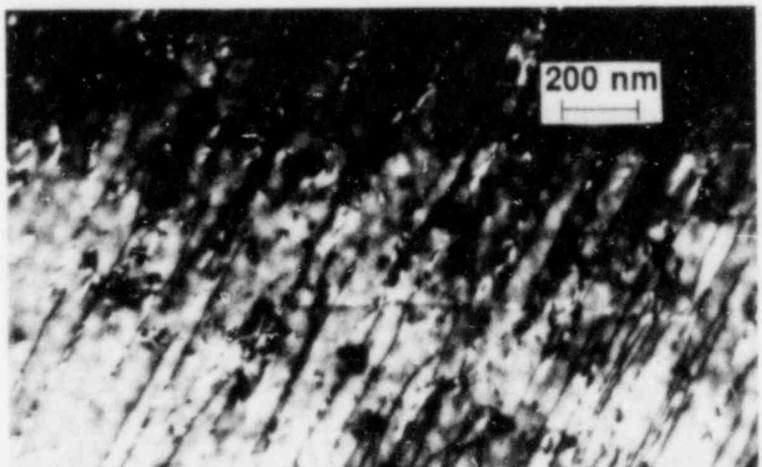


Fig. 13. Dark-Field Image Showing Light Type X Precipitates Interwoven with Dislocations in the Ferrite Phase of the Reactor Pump Cover Material.

## 2. Precipitate Characterization by Small-Angle Neutron Scattering

Although the very fine α' in the GF materials, aged either at 300°C for 8 yr or at 400°C for 7.6 yr, could be resolved by the weak-beam TEM technique, the results from the small-angle neutron scattering experiments showed no distinct intensity peak at ~1-nm diameter, which corresponds to the size of α' in the materials. However, an intensity peak corresponding to the G-phase, which exhibits a distinct phase boundary (relative to the ferrite matrix) and a size an order of magnitude larger than the α', was observed as shown in Fig. 15.[14] The diameters of the most populous scattering centers shown in Figs. 15(A) and (B), i.e., ~1.6 and ~5.5 nm, are in good agreement with the sizes of the G-phase observed by TEM for the two aging conditions, i.e., GF Heat 278 aged at 400°C for 1.2 and 7.8 yr, respectively. A comparison of Figs. 15(A) and (B) shows an Ostwald ripening of the G-phase after aging at 400°C for 7.6 yr. The absence of an intensity peak corresponding to the α' size (1-2 nm) in Fig. 15 is not surprising since a distinct phase boundary is not expected between the chromium-rich α' and chromium-depleted ferrite phase in the materials.

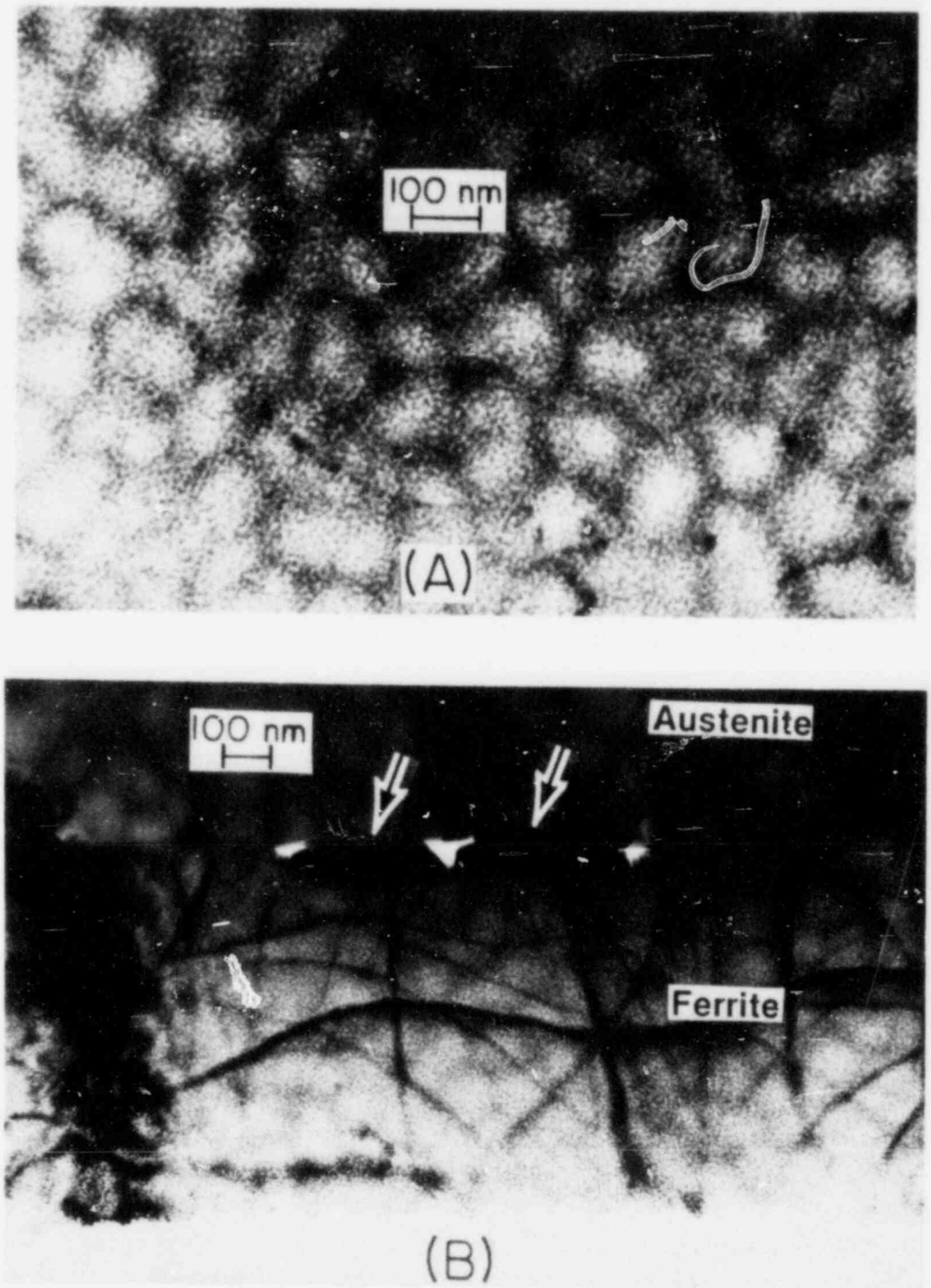


Fig. 14. Morphologies of α' Observed in the Ferrite Phase of the Reactor Pump Cover (A) and Heat 60 Cast-Duplex Stainless Steel after Aging at 400°C for 10,000 h (B). $M_{23}C_6$ precipitates on the phase boundary are denoted by arrows in (B).

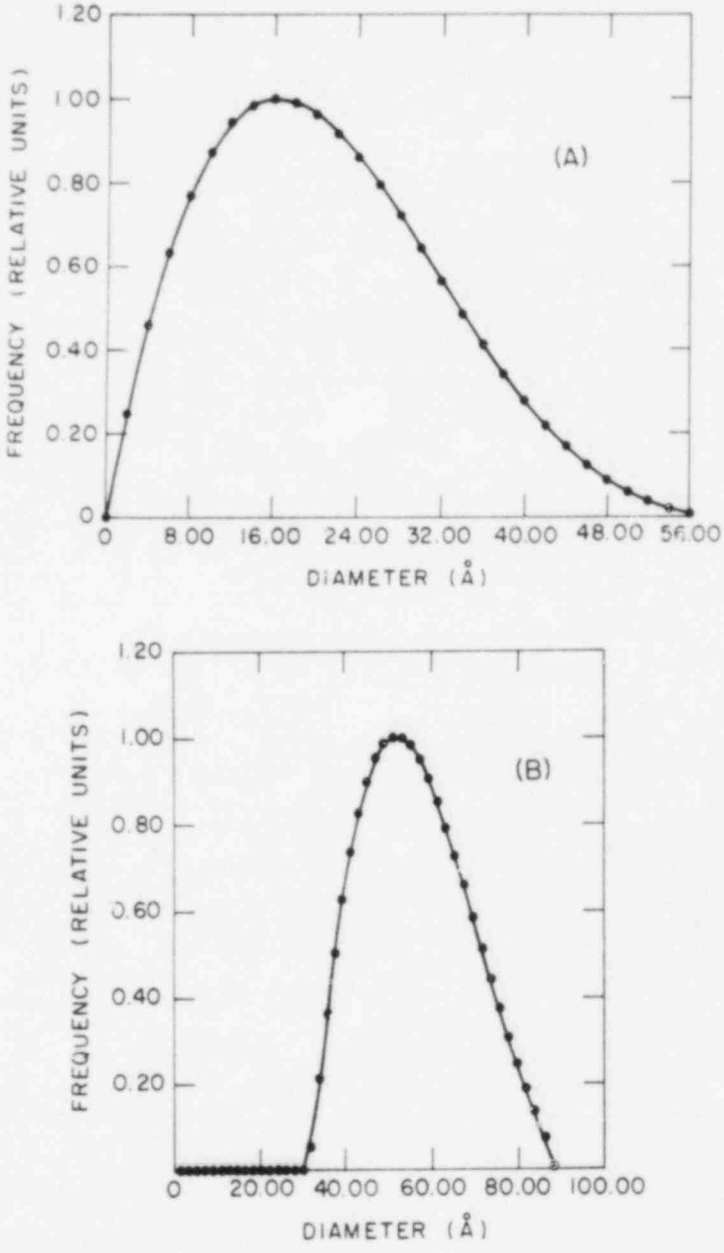


Fig. 15. Relative Population of Precipitates vs Guinier Diameter Obtained by Small-angle Neutron Scattering Technique for the G. Fischer Cast-Duplex Stainless Steel Heat 278 after Aging at 400°C for 1.2 yr (A) and 7.6 yr (B).

### 3. Grain Boundary Precipitate

A distinct difference between the microstructures of the laboratory-aged GF materials and the reactor pump-cover material involves precipitation of a grain boundary phase in the latter. Bright- and dark-field morphologies and an SAD pattern of the grain boundary phase are shown in Fig. 16. The phase was observed on the boundary between the austenite and ferrite grains, examples of which appear as the dark and light areas, respectively, in Fig. 16(A). Several different zone axes similar to that of the SAD pattern in Fig. 16(C) were obtained. Indexing of the diffraction patterns showed that the grain boundary precipitates were $M_{23}C_6$ carbides, which were of cube-on-cube orientation relative to austenite. The overall distribution of the grain boundary phase could be more clearly observed in low-magnification optical micrographs. For example, in Fig. 16(D), ~60% of the austenite-ferrite grain boundaries are decorated by the phase; this observation indicates a possible weakening of the grain boundaries. The lacy morphology of the ferrite is evident from Fig. 16(D). Aging of Heat 60 also yielded grain boundary precipitation of the $M_{23}C_6$ carbide, Fig. 14(B). The chemical composition of Heat 60 is very similar to that of the reactor pump material. However, the grain boundary $M_{23}C_6$ carbide was not observed in the low-carbon Heat 51 after aging at 400°C for ~1.2 yr. The absence of grain-boundary carbide precipitates in Heat 51 and the GF materials, i.e., Heats 280 and 278, is most likely related to the low-carbon contents (Table 3) compared to the higher carbon contents of the reactor pump and Heat 60 materials.

The precipitation of grain boundary carbides appears to be responsible for the rapid reduction in the impact energy for the high-carbon Heat 60 compared to that for Heat 51 [Fig. 11(a)]. However, the microstructural characteristics of the ferrite matrix are similar for the two heats and, as expected, the hardnesses of the ferrite phase are comparable [Fig. 11(b)]. The grain-boundary $M_{23}C_6$ precipitation in Heat 60 was significantly smaller after aging at 350°C for 10,000 h than after aging at 400°C for similar times. This is believed to be one of the factors which contribute to the higher impact energies for Heat 60 aged at 350°C relative to those aged at higher temperatures. However, the lower hardness of the ferrite phase for the

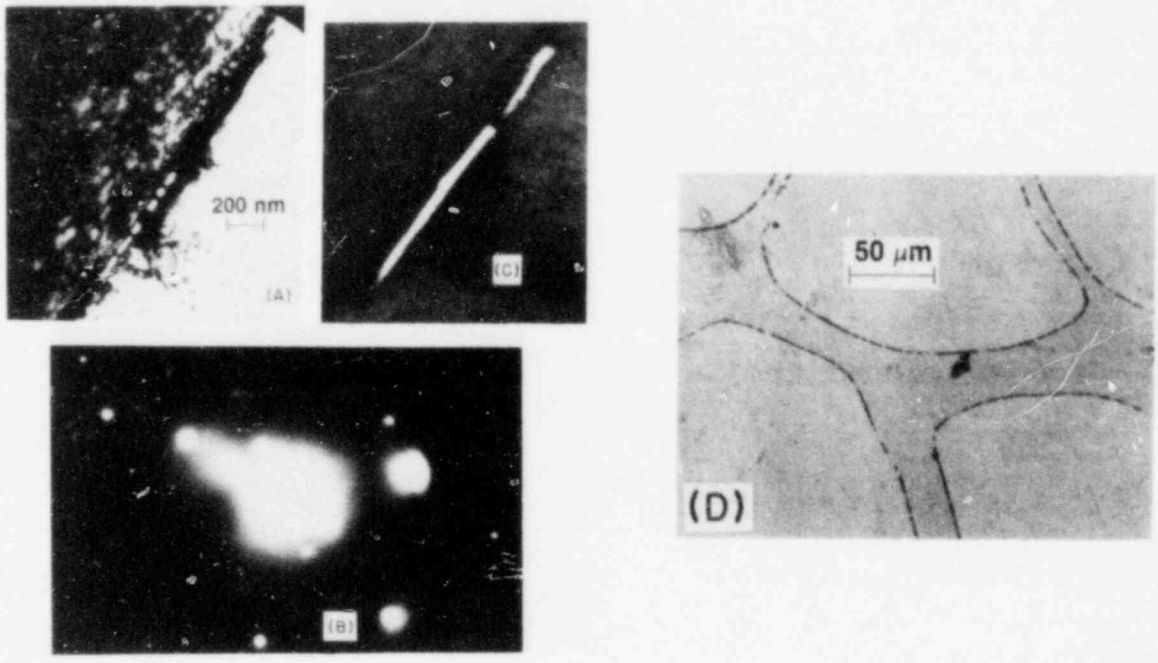


Fig. 16. Bright-Field (A) and Dark-Field (B) Images, SAD Pattern (C), and an Optical Micrograph (D) of $M_{23}C_6$ Grain Boundary Precipitates Observed in the Reactor Pump Cover Material.

material aged at 350°C indicates that other factors, viz., microstructural characteristics of the ferrite matrix, also contribute to the overall embrittlement behavior.

4. SEM Fractography

Fracture surface morphologies of the laboratory-aged GF materials and the reactor pump-cover material were evaluated by SEM after room-temperature impact tests. The fracture surface morphology of the ferrite phase of the reactor pump cover and the GF material aged at 300°C for 8 yr or at 400°C for 1.2 yr was invariably cleavage-type (Fig. 17), which means negligible ductility of the phase. Undoubtedly, the ferrite was generally embrittled by one or combinations of the above-mentioned precipitates, i.e., G-phase, Type X, and α'. It was, in fact, possible to map the cleavage-ferrite and ductile-austenite portions of a given fracture surface. The cleavage map of the reactor pump cover indicated that ~50-60% of the overall fracture surface was ferrite, although the ferrite volume fraction was only ~30%. Although not conclusive, this finding indicates preferential crack

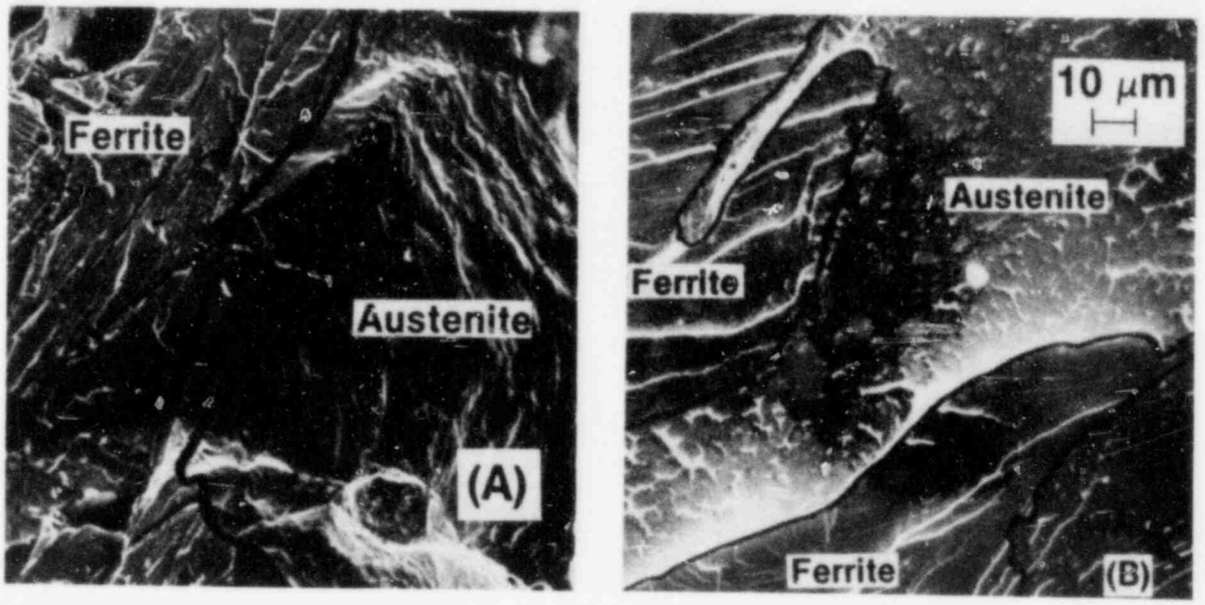


Fig. 17. Fracture Surface Morphologies of the Room-Temperature Impact-tested Specimens of the G. Fischer Material Aged at 300°C for 8 yr (A) and the Reactor Pump Cover Material after 12 yr of Service in a Boiling-Water Reactor (B).

propagation along the ferrite phase under the impact condition. There was also some indication of decohesion along the grain boundary of the reactor pump-cover material, as shown in Fig. 17(B). The relatively smooth morphology shown in Fig. 17(B) appears to correspond to grain boundaries that are partly covered by ductile tears. This observation is consistent with the microstructures of Fig. 16, in which a significant fraction of the grain boundaries was covered by the carbide precipitates. However, for the laboratory-aged GF materials, the austenite fracture surface morphology invariably showed transgranular ductile failures, as in Fig. 17(A). The intergranular decohesion of aged cast-duplex stainless steel, associated with the austenite/ferrite boundary carbide precipitate, appears to have been observed also elsewhere.[15]

## III. CONCLUSIONS

Data from room-temperature impact tests and microstructural characterization indicate that the existing correlations do not accurately represent the embrittlement behavior of cast-duplex stainless steels over the temperature range of 300-450°C. The carbon content in the steel may be an important factor in controlling the overall process of embrittlement, particularly at

temperatures $\geq$400°C. Preliminary results suggest that at least two processes contribute to the embrittlement of duplex stainless steels, viz., weakening of the ferrite/austenite phase boundary by carbide precipitation, and embrittlement of ferrite matrix by the formation of additional phases such as G-phase, Type X, or the $\alpha'$ phase. The latter occurs in all heats of cast stainless steels and is primarily responsible for embrittlement of low-carbon materials (i.e., CF-3 grade) at temperatures below 350°C. However, the relative importance of the three precipitates under different compositional and aging conditions cannot be quantitatively established at this time. The precipitation of $M_{23}C_6$ carbides at the ferrite/austenite phase boundary has a significant effect on embrittlement of high-carbon materials, i.e., grade CF-8. Carbide precipitation dominates the onset of embrittlement of cast CF-8 or -8M stainless steels aged at 400 or 450°C. Charpy-impact and microstructural data will be obtained on materials aged at temperatures between 290 and 350°C for long times to evaluate the relative contribution of the different precipitation processes on embrittlement of cast-duplex stainless steels.

## ACKNOWLEDGMENTS

The authors acknowledge the experimental contributions provided by L. P. Burkel and metallography and scanning electron microscopy performed by R. A. Conner, Jr. and G. M. Dragel. This work was supported by the U. S. Nuclear Regulatory Commission, Office of Nuclear Regulatory Research, under Contract W-31-109-Eng-38. The authors wish to thank W. J. Shack and J. Muscara for their helpful discussions.

## REFERENCES

1. A. Trautwein and W. Gysel, "Influence of Long Time Aging of CF-8 and CF-8M Cast Steel at Temperatures Between 300 and 500 deg. C on the Impact Toughness and the Structure Properties," Spectrum, Technische Mitteilungen aus dem+GF+Konzern, No. 5 (May 1981); Stainless Steel Castings, eds. V. G. Behal and A. S. Melilli, ASTM STM 756 (1982), p. 165.

2. O. K. Chopra and G. Ayrault, Long-Term Embrittlement of Cast Duplex Stainless Steels in LWR Systems: Annual Report, October 1982-September 1983, NUREG/CR-3857, ANL-84-44 (July 1984); Nucl. Eng. Des. 86, p. 69 (1985).

3. O. K. Chopra and H. M. Chung, in Materials Science and Technology Division Light-Water-Reactor Safety Research Program: Quarterly Progress Report, October-December 1984, NBUREG/CR-3998 Vol. III, ANL-84-60 Vol. III (October 1985), pp. 48-61.

4. O. K. Chopra and G. Ayrault, in Materials Science and Technology Division Light-Water-Reactor Safety Research Program: Quarterly Progress Report, October-December 1983, NUREG/CR-3689 Vol. IV, ANL-83-85 Vol. IV (August 1984), pp. 129-151.

5. O. K. Chopra and H. M. Chung, in Materials Science and Technology Division Light-Water-Reactor Safety Materials Engineering Research Programs: Quarterly Progress Report, January-March 1984, NUREG/CR-3998 Vol. I, ANL-84-60 Vol. I (September 1984), p. 52.

6. O. K. Chopra and H. M. Chung, Long-Term Embrittlement of Cast Duplex Stainless Steels in LWR Systems: Annual Report, October 1983-September 1984, NUREG/CR-4204, ANL-85-20 (March 1985).

7. G. Slama, P. Petrequin, and T. Magep, "Effect of Aging on Mechanical Properties of Austenitic Stainless Steel Castings and Welds," presented at SMIRT Post-Conference Seminar 6, Assuring Structural Integrity of Steel Reactor Pressure Boundary Components, August 29 and 30, 1983, Monterey, CA.

8. H. M. Chung and O. K. Chopra, "Microstructure of Cast-Duplex Stainless Steel after Long-Term Aging," in Proc. Second Intl. Symp. on Environmental Degradation of Materials in Nuclear Power Systems - Water Reactors, September 9-12, 1985, Monterey, CA, to be published.

9. G. T. Brown and R. T. Allsop, "Embrittlement of a 12%Cr-4Ni Steel," J. Iron Steel Inst. (1960), p. 435.

10. D. S. Gelles and L. E. Thomas, "Effects of Neutron Irradiation on Microstructure in Commercial and Experimental Ferritic Alloys," presented at Topical Conf. on Ferritic Alloys for Use in Nuclear Energy Technologies, June 19-23, 1983, Snowbird, UT.

11. M. K. Miller, J. Bentley, S. S. Brenner, and J. A. Spitznagel, "Long Term Thermal Aging of Type CF-8 Stainless Steel," J. Phys. (Paris) Colloq. 45 (1984), p. C9-835.

12. J. Bentley, M. K. Miller, S. S. Brenner, and J. A. Spitznagel, "Identification of G Phase in Aged Cast CF-8 Type Stainless Steel," in Proc. of the 43rd Annual Meeting of the Electron Microscopy Society of America, G. W. Bailey, ed. (1985), p. 328.

13. D. J. H. Cockayne, "The Weak-Beam Method of Electron Microscopy," in Diffraction and Imaging Techniques in Material Science, S. Amelinckx, R. Gevers, and J. Van Landuyt, eds., North Holland, 1978, Vol. I, pp. 153-183.

14. J. E. Epperson, J. S. Lin, and S. Spooner, "The Fine Scale Microstructure in Cast and Aged Duplex Stainless Steels Investigated by Small Angle Neutron Scattering," to be published.

15. J. R. Donati, Electricité de France, France, private communication.

Distribution for NUREG/CR-4503 (ANL-86-3)

Internal:

R. Avery
G. Ayrault
O. K. Chopra (5)
H. M. Chung (3)
D. R. Diercks
F. Y. Fradin
T. F. Kassner (5)
K. L. Kliewer
D. S. Kupperman
F. A. Nichols
J. Y. Park
W. J. Shack (3)
W. K. Soppet
E. M. Stefanski (2)
C. E. Till
R. A. Valentin
R. W. Weeks
H. Wiedersich
R. S. Zeno
ANL Patent Dept.
ANL Contract File
ANL Libraries (2)
TIS Files (5)

External:

NRC, for distribution per R5 (350)
DOE-TIC (2)
Manager, Chicago Operations Office, DOE
R. X. Tom, DOE-CH
Materials Science and Technology Division Review Committee:
C. B. Alcock, U. Toronto
A. Arrott, Simon Fraser U.
R. C. Dynes, AT&T Bell Labs., Murray Hill
A. G. Evans, U. California, Berkeley
H. K. Forsen, Bechtel National, Inc., San Francisco
E. Kay, IBM San Jose Research Lab.
M. B. Maple, U. California, San Diego
P. G. Shewmon, Ohio State U.
J. K. Tien, Columbia U.
J. W. Wilkins, Cornell U.
G. A. Arlotto, Office of Nuclear Regulatory Research, USNRC, Washington
D. Atteridge, Battelle Pacific Northwest Lab., P. O. Box 999, Richland, Wash. 99352
W. H. Bamford, Westinghouse Electric Corp., WNES, Box 355, Pittsburgh, Pa. 15230
C. Y. Cheng, Office of Nuclear Reactor Regulation, USNRC, Washingon
W. J. Collins, Office of Inspection and Enforcement, USNRC, Washington
A. Cowan, Risley Nuclear Power Development Labs., UKAEA (Northern Div.), Risley, Warrington WA3 6AT, U. K.
W. H. Cullen, Materials Engineering Associates, Inc., 9700 B. George Palmer Highway, Lanham, Md. 20706
B. J. L. Darlaston, CEGB, Berkeley Nuclear Laboratories, Berkeley, Glos., U. K.
B. J. Elliot, Office of Nuclear Reactor Regulation, USNRC, Washington
W. Gysel, Georg Fischer, Ltd., Schaffhausen, Switzerland
W. S. Hazelton, Office of Nuclear Reactor Regulation, USNRC, Washington
B. Hemsworth, HM Nuclear Installations Inspectorate, Thames House North, Millbank, London SW1P 42J, U. K.
W. V. Johnston, Office of Nuclear Reactor Regulation, USNRC, Washington
D. de G. Jones, Materials Science Div., Atomic Energy Corp., Private Bag X256, Pretoria 0001, South Africa
P. M. Lang, Office of Converter Reactor Deployment, USDOE, Washington
J. Muscara, Office of Nuclear Regulatory Research, USNRC, Washington
D. M. Norris, Electric Power Research Inst., P. O. Box 10412, Palo Alto, Calif. 94303
C. Z. Serpan, Office of Nuclear Regulatory Research, USNRC, Washington
V. K. Sikka, Oak Ridge National Lab., P. O. Box X, Oak Ridge, Tenn. 37830

G. Slama, Framatome, Tour FIAT, Cedex 16, 92084 Paris La Defense, France
P. Smerd, Combustion Engineering, Inc., P. O. Box 500, Windsor, Conn. 06095
H. D. Solomon, General Electric Co., P. O. Box 43, Schenectady, N. Y. 12301
D. M. Stevens, Lynchburg Research Center, Babcock & Wilcox Co., P. O. Box 239, Lynchburg, Va. 24505

NRC FORM 336 (2-84) NRCM 1102 3201 3202

U.S. NUCLEAR REGULATORY COMMISSION

**BIBLIOGRAPHIC DATA SHEET**

SEE INSTRUCTIONS ON THE REVERSE

1. REPORT NUMBER (Assigned by TIDC and Vol. No. if any)

NUREG/CR-4503
ANL-86-3

2. TITLE AND SUBTITLE

Long-term Embrittlement of Cast-Duplex Stainless Steels in LWR Systems: Annual Report, October 1984-September 1985

3. LEAVE BLANK

4. DATE REPORT COMPLETED

MONTH: January YEAR: 1986

5. AUTHOR(S)

O. K. Chopra and H. M. Chung

6. DATE REPORT ISSUED

MONTH: January YEAR: 1986

7. PERFORMING ORGANIZATION NAME AND MAILING ADDRESS (Include Zip Code)

Argonne National Laboratory
9700 South Cass Avenue
Argonne, Illinois 60439

8. PROJECT/TASK/WORK UNIT NUMBER

9. FIN OR GRANT NUMBER

A2243

10. SPONSORING ORGANIZATION NAME AND MAILING ADDRESS (Include Zip Code)

U. S. Nuclear Regulatory Commission
Office of Nuclear Regulatory Research
Washington, D. C. 20555

11a. TYPE OF REPORT

Annual Report

b. PERIOD COVERED (Inclusive dates)

October 1984-September 1985

12. SUPPLEMENTARY NOTES

13. ABSTRACT (200 words or less)

This progress report summarizes work performed by Argonne National Laboratory during the twelve months from October 1984 to September 1985 on long-term embrittlement of cast-duplex stainless steels used in light-water reactors.

14. DOCUMENT ANALYSIS - a. KEYWORDS/DESCRIPTORS

Cast stainless steels
Embrittlement behavior
Low-temperature aging
Phase precipitation and identification

b. IDENTIFIERS/OPEN-ENDED TERMS

15. AVAILABILITY STATEMENT

Unlimited

16. SECURITY CLASSIFICATION

(This page) Unclassified

(This report) Unclassified

17. NUMBER OF PAGES

38

18. PRICE

120555078877 1 1AN1R5
US NRC
ADM-DIV OF TIDC
POLICY & PUB MGT BR-PDR NUREG
W-501
WASHINGTON DC 20555